Scripta Materialia 153 (2018) 40–43

Contents lists available at ScienceDirect

Scripta Materialia

journal homepage: www.elsevier.com/locate/scriptamat

Regular Article

Rare earth-free hard magnetic microwires

I. Betancourt [a,*], J. Zamora [a,b], A. Jiménez [b], R.P. del Real [b], M. Vázquez [b]

[a] Instituto de Investigaciones en Materiales, Universidad Nacional Autónoma de México, Ciudad de México CP 04510, Mexico
[b] Instituto de Ciencia de Materiales de Madrid, CSIC, Sor Juana Inés de la Cruz 3, 28049 Madrid, Spain

ARTICLE INFO

Article history:
Received 12 March 2018
Received in revised form 24 April 2018
Accepted 25 April 2018
Available online 21 May 2018

Keywords:
Magnetic microwires
Hard magnetic properties
High coercivity alloys

ABSTRACT

Novel microwires of composition MnBi were obtained by means of quenching and drawing technique having a metallic nucleus of 50 μm diameter. Phase distribution analysis showed a composite microstructure comprising extensive zones of the ferromagnetic hexagonal MnBi phase (of up to 12 μm), interspersed within a matrix of diamagnetic Bi and some inclusions of pure Mn varying between 1 and 2 μm in length. A coercive field in excess of 4000 Oe was measured. Coercivity mechanism is described in terms of nucleation of reverse domains, for which the interface MnBi/Bi largely determines the hard magnetic response of the composite microwire.

Magnetic microwires prepared by quenching and drawing technique has been intensively studied since 20 years ago due to their remarkable soft magnetic behavior, characterized by small coercivity H_c values (<1 Oe), high magnetic permeability (>10,000) and vanishing magnetocrystalline anisotropy K_1 (≈0 for amorphous alloys), as well as properties of practical interest such as magnetomechanical and giant magnetoimpedance effects [1–3]. These characteristics enable them for an ample variety of potential applications such as micro- and nano-electronics systems, miniaturized sensor and actuators [4]. Typically, these types of microwires include a metallic nucleus of variable diameter ranging 1–30 μm, covered by an insulating layer of pyrex glass (2–10 μm thick) [5]. Base composition to obtain glass-coated microwires with amorphous microstructure and soft magnetic response includes combination of transition metals (Fe, Co, Ni) and metalloids like B and Si. The strong chemical affinity between the transition metal and the metalloid species promotes high glass forming ability for these alloys and thus, the solidification of amorphous solids. Nanocrystalline microwires with semi-hard magnetic response (H_c ≈ 80 Oe) have also been reported for Fe-based compositions, as a consequence of annealing process above 600 °C, which causes the precipitation of a second crystalline phase (γ-Fe) [6]. Microwires with granular microstructure can also be obtained from immiscible elements such as (Co, Fe, Ni) and (Pt, Au, Ag, Cu) [7,8]. These immiscible alloys exhibit peculiar magnetic properties such as the giant magnetoresistance effect associated with ferromagnetic nanoclusters embedded in a diamagnetic matrix [9]. Enhanced H_c (about 100 Oe and above) are also possible after recrystallization process [10,11]. Up to now, glass-coated microwires with hard magnetic behavior (i.e., with coercivity values over 100 Oe) have not yet been reported.

On the other hand, research on hard magnetic alloys with rare earth-free compositions has elicited a significant interest recently due to the possibility for developing competitive permanent magnets alternative to rare-earth based compositions such as NdFeB-based or SmCo supermagnets. In particular, MnBi alloys with hexagonal P63/*mmc* structure attracts attention due to their characteristic Low Temperature Intermetallic Phase (LTIP) possessing a suitable combination of intrinsic magnetic properties including high K_1 (of 1×10^7 erg/cm^3), intermediate saturation magnetization M_s (7300 G) and high Curie transition T_c (of 345 °C).

A variety of methods have been explored for obtaining alloys with LTIP, such as arc-melting, powder metallurgy, mechanical milling, melt-spinning and induction furnace [12–15], for which coercive fields varying within the range 50 Oe – 12,000 Oe were reported, alongside saturation magnetization between 0.1 T and 0.7 T. In general, for all these methods, a subsequent heat treatment is required to complete the formation of the LTIP. A different approach based on metal-redox method to synthesize single-domain MnBi nanoparticles stable in air resulted in nanoparticles with average size below 300 nm, for which a remarkable coercive field of 14,000 Oe was measured [16].

In this work, we exploit the specific characteristics of ultrafast fabrication process, as quenching and drawing technique, to introduce novel microwires with MnBi composition, as well as to explore and discuss their hard magnetic response.

Initial ingots of $Mn_{0.5}Bi_{0.5}$ alloy were prepared by means of arc-melting of elemental constituents in a titanium-gettered inert atmosphere. The samples were remelted at least five times at temperatures over 2500 °C to ensure chemical uniformity. From the master ingots, pieces of glass-coated microwires were obtained by quenching and

* Corresponding author.
E-mail address: israelb@unam.mx (I. Betancourt).

https://doi.org/10.1016/j.scriptamat.2018.04.045
1359-6462/

drawing technique with the following dimensions: 50 μm diameter for the metallic core, 18 μm for the glass coating and variable lengths from 2 to 4 mm up to 2–4 cm. Phase distribution analysis was carried out by X-ray diffraction (XRD) using a Siemens D5000 diffractometer with Co-Ka radiation (λ = 1.7903 angstrom) and a step size of 0.020°. Microstructural analysis was performed by a Field Emission Scanning Electron Microscopy (FESEM) in a JEOL 7600F equipment. Magnetic measurements were realized by Vibrating Sample Magnetometer (VSM) in a MPMS system with a maximum applied field of 30,000 Oe and variable temperature within the range 200 K–360 K.

Phase distribution analysis performed by means of X-ray diffractograms (not shown) afforded the identification of two main constituent phases: pure Bi and the LTIP-MnBi, according to ICDD files 044-1246 and 03-065-8733, respectively. Segregation of pure Bi is favored by the high cooling rate of the casting process, which hinders atomic diffusion, as well as to the peritectic reaction through which the formation of the LTIP occurs, which also promotes separation of atomic species.

Field Emission Scanning Electron Microscopy (FESEM) micrographs are shown in Fig. 1a for the MnBi microwire. The use of backscattered electrons allows one to identify three zones with different contrast, and thus, variable chemical composition: dark precipitates dispersed between gray and light gray zones. According to EDS data collected from each zone, the corresponding phases are: pure Mn (dark precipitates), LTIP-MnBi (gray zones) and pure Bi (light gray areas). LTIP zones present lengths between 1.0 and 12.0 μm, whereas Mn crystals showed variable lengths within the range 1.0–2.5 μm. No inner inclusions within LTIP zones are visible. The areas of pure Bi exhibit variable extension, from 1.0 to 15.0 μm. The formation of well-defined Mn structures is evidenced in Fig. 1b, for which faceted crystals are clearly visible.

The hysteresis curve for the MnBi microwire is displayed in Fig. 2a, for which the following magnetic properties were determined: maximum magnetization $M_m = 57.5$ emu/cm^3, remanence magnetization $M_r = 27.3$ emu/cm^3 and a noticeable coercive field $H_c = 4610$ Oe. The irreversible region reaches up to an applied field of around 15,000 to 2000 Oe. This combination of properties reflects the hard magnetic character of the MnBi microwire.

The initial magnetization curve for MnBi microwire is displayed in Fig. 2b, for which the steep slope at the onset of the curve, associated to the initial magnetic susceptibility, can be interpreted as reflecting a relatively easy displacement of domain walls within the magnetic LTIP zones due to the absence of inner inclusions (i.e., pining centers), such as described in Fig. 1. This feature suggests the nucleation of reverse domains (after saturation) as the active coercivity mechanism for this alloy.

Complementary measurements of the temperature dependence of M_m and H_c are displayed in Fig. 3. The maximum magnetization decreases as the temperature T increases (Fig. 3a), whereas H_c increases for increasing temperature (Fig. 3b) due to the characteristic increase of the magnetocrystalline anisotropy of the LTIP phase [17]. Though the magnetic properties of present MnBi microwires lie within the average intervals reported for bulk or melt spun alloys, the fact that coercive field increases with increasing temperature, together with their particular microsized cylindrical geometry, renders this material as an ideal candidate for magnetic element of microsystems technology, for which application of magnetic components includes sensors, passive devices (such as inductors and transformers) and actuators based on

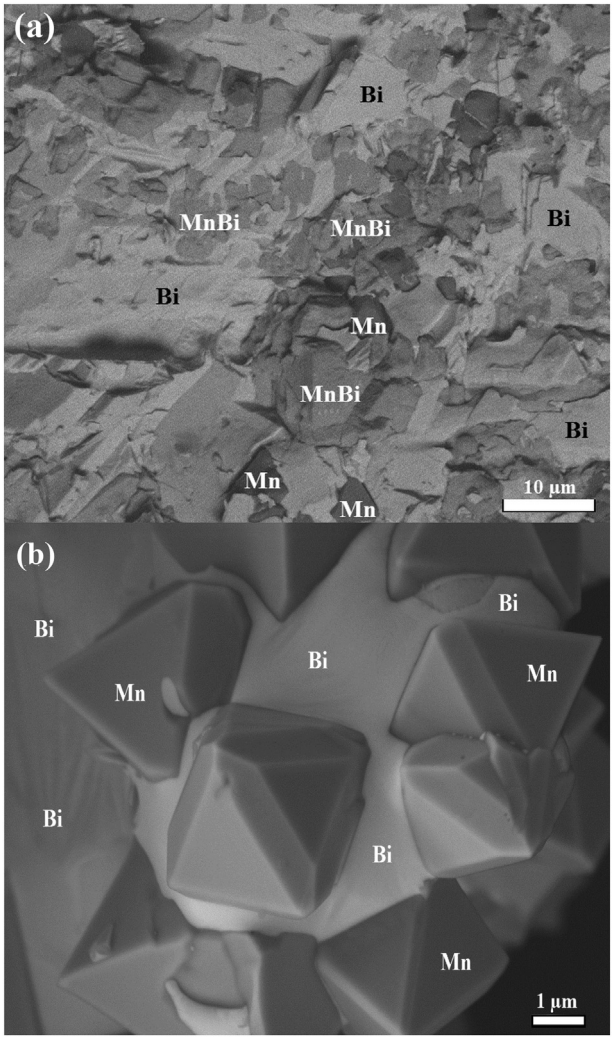

Fig. 1. FESEM micrograph for the MnBi microwire showing a) phase distribution comprising Mn precipitates, LTIP-MnBi zones and pure Bi areas b) amplification of Mn crystals showing faceted structure.

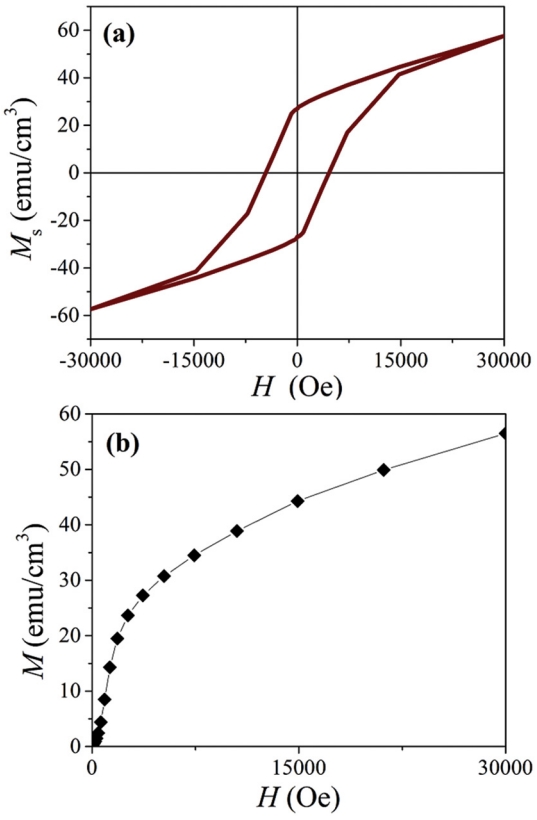

Fig. 2. Magnetization curve for the MnBi microwire a) Hysteresis plot b) initial magnetization curve.

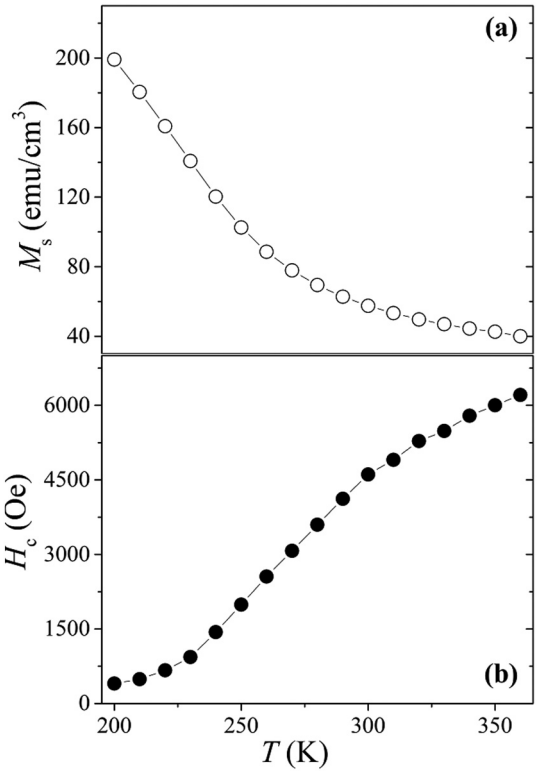

Fig. 3. Temperature dependence for a) maximum magnetization and b) coercive field of the MnBi microwire.

magnetic interactions, such as attenuators, micro-relays, micromotors, micropumps, and magnetic energy harvester [18].

Within the frame of the nucleation controlled coercivity mechanism, the development of high values for coercivity field H_c relies on the nucleation field necessary for the onset of magnetization reversal taking place at the interface of defects, non-magnetic grains or significant misalignment between magnetic grains. According to Kronmüller [19,20], in order to incorporate the detrimental influence of microstructural defects in real materials (point defects, grain boundaries, non-magnetic phases) the equation for H_c is given by

$$\mu_0 H_c = \mu_0 H_N^{min} \alpha_K - N_{eff}(\mu_0 M_s) \quad (1)$$

where H_N^{min} stands for the minimum nucleation field ($H_N^{min} = K_1/M_s$), α_K is a microstructural parameter representing the reduction of K_1 at the surface interfaces with non-magnetic regions and N_{eff} is an average effective demagnetization factor describing the internal stray fields acting on the grains. In order to fit experimental data of Fig. 3 with Eq. (1), it is necessary to plot

$$\frac{\mu_0 H_c}{\mu_0 M_m}(T) \text{ vs } \frac{K_1}{\mu_0 M_s^2}(T) \quad (2)$$

where the left hand side corresponds to experimental data for H_c (T) and M_m (T) (Fig. 3), whereas the right hand side corresponds to the temperature dependences of the intrinsic magnetic parameters K_1 and M_s for the MnBi LTIP reported in [17]. The fitting of experimental data to expression (2) is shown in Fig. 4, for which a linear tendency is manifested for the temperature interval 240–360 K.

From the fitting process, we obtain $\alpha_K = 0.32$ and $N_{eff} = 1.17$ as the slope and the ordinate intersection of the straight line. Very similar α_K, N_{eff} parameters were reported for equivalent MnBi alloys characterized by Kronmüller et al. [21] ($\alpha_K = 0.3$ $N_{eff} = 0.75$) and Curcio et al. [22] ($\alpha_K = 0.31$ $N_{eff} = 2.01$). According to Kronmüller et al. [21], an $\alpha_K = 0.3$ for

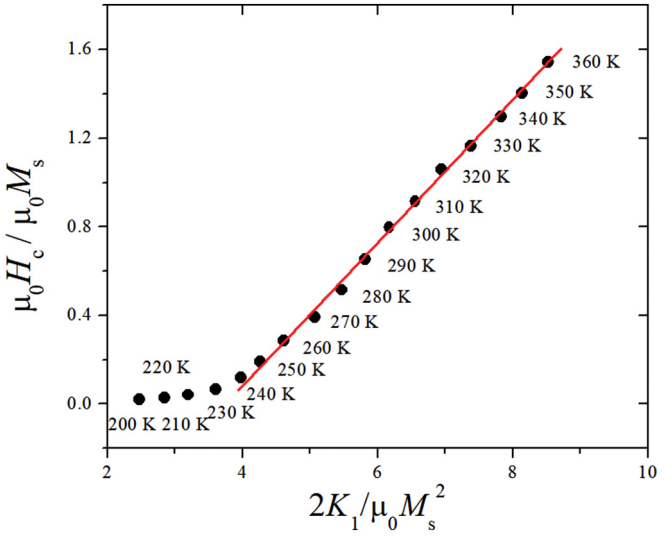

Fig. 4. Fitting of experimental data for Eq. (1) ($R^2 = 0.998$).

nanostructured MnBi alloys implies a deteriorated surface region of 3.3 nm, where the magnetocrystalline anisotropy reduces in a significant way yielding to low $\mu_0 H_N$ and hence, low $\mu_0 H_c$ values. The deviation from linear tendency in Fig. 4 at low temperature (<250 K) reflects a change of coercivity mechanism for wider domain walls (promoted by reduced values of K_1 at low temperature for the LTIP [17]). This low temperature deviation is also manifested at the M_m (T) curve of Fig. 4, for which other reports ascribe to a magnetic transition of the spin reorientation-type [23–25].

In order to achieve materials with high coercive fields, it is necessary to combine high magnetic anisotropy and a propitious microstructure. For the present MnBi microwires, we have a considerable magnetocrystalline anisotropy given by $K_1 = 1.0$ MJ/m^3 [25] whereas the critical microstructure feature is the excess of Bi content which segregates as a boundary phase separating ferromagnetic LTIP zones. This matrix of diamagnetic Bismuth promotes the magnetostatic interaction between LTIP areas, as suggested by the Henkel plot δM (included as supplementary material), for which only a negative portion of the curve is visible, which is consistent with a predominant long-range interaction of magnetostatic nature [26–29].

The onset of reversal of magnetization occurs at the MnBi-Bi/MnBi-Mn interfaces, where a significant reduction of K_1 is expected due to the non-magnetic nature of Bi as well as to the cubic crystal structure of Mn. In addition, sharp edges of LTIP zones are also present (see Fig. 1a), which in turn also favors the reversal of magnetization and thus, a reduced coercivity value relative to the expected nucleation field $H_N = 2\ K_1/M_s = 30{,}800$ Oe of the MnBi-LTIP. This H_N states a theoretical maximum coercivity for ideal materials (Brown paradox) [19,30].

Hard magnetic properties were found for novel MnBi alloys in the shape of microwires obtained by quenching and drawing technique, characterized by a coercive field in excess of 4000 Oe for which a nucleation-controlled mechanism was described. The presence of pure Bi as non-magnetic phase interspersed among ferromagnetic LTIP regions zones determines the development of the observed high coercivity of the studied microwires.

Acknowledgment

I·Betancourt acknowledges financial support from research project UNAM-PAPIIT IN103216. J. Zamora is grateful for the scholarship received from UNAM-PAPIIT IN103216 and CONACYT-Mexico. Special thanks are given to Adriana Tejeda, Omar Novelo and Josue Romero (IIM-UNAM) for their valuable technical assistance. The work has been

partly supported by the Regional Government of Madrid under Project S2013/MIT-1942850, NANOFRONTMAG-CM.

Appendix A. Supplementary data

Supplementary data to this article can be found online at https://doi.org/10.1016/j.scriptamat.2018.04.045.

References

[1] M. Vázquez, in: H. Kronmüller, S. Parkin (Eds.), Handbook of Magnetism and Advanced Magnetic Materials, Vol. 4, Wiley, New York 2007, pp. 2193–2226.
[2] A. Zhukov, J. Gonzalez, M. Vazquez, V. Larin, A. Torcunov, in: H.S. Nalwa (Ed.), Encyclopedia of Nanoscience and Nanotechnology, American Scientific Publishers, New York 2004, p. 23 (Chapter 62).
[3] M. Vázquez, Physica B 299 (2001) 302–313.
[4] M. Vazquez (Ed.), Magnetic Nano- and Microwires, Woodhead Publishing, Cambridge, UK, 2015.
[5] T.A. Ovari, S. Corodeanu, H. Chiriac, J. Appl. Phys. 109 (2011) (07D502).
[6] J. Gonzalez, Zhukov, V. Zhukova, A.F. Cobeño, J.M. Blanco, A.R. De Arellano-Lopez, S. Lopez-Pombero, J. Martinez-Fernandez, V. Larin, A. Torcunov, IEEE Trans. Magn. 36 (2000) 3015.
[7] A. Zhukov, E. Sinnecker, D. Paramo, F. Guerrero, V. Larin, J. Gonzalez, M. Vázquez, J. Appl. Phys. 85 (1999) 4482–4484.
[8] C.L. Chen, J.Q. Xiao, J.S. Jiang, J. Appl. Phys. 73 (1993) 5309.
[9] S.F. Marenkin, A.D. Izotov, V.M. Novotortsev, Proceedings of the International Conference Topics in Solid State Physics (Minsk, 2013), 1 (56) (2013).
[10] J. Gonzalez, V. Zhukova, A.P. Zhukov, J.J. del Val, E. Pina, M. Vazquez, J. Magn. Magn. Mater. 221 (2000) 196–206.
[11] J.M. González, A. Hernando Mañeru, F. Cebollada, J.J. del Val, A.P. Zhukov, IEEE International Magnetics Conference (INTERMAG) Amsterdan, 2002 GC07.
[12] H. Yoshida, T. Shima, T. Takahashi, H. Fujimori, Mater. Trans. JIM 40 (1999) 455–458.
[13] F. Yin, N. Gu, J. Mater. Sci. Technol. 12 (1996) 335–341.
[14] K. Isogai, M. Matsuura, N. Tezuca, S. Sugimoto, Mater. Trans. JIM 54 (2013) 1673–1677.
[15] T. Saito, R. Nishimura, D. Nishio-Hamane, J. Magn. Magn. Mater. 349 (2014) 9–14.
[16] A. Kirkeminde, J. Shen, M. Gong, J. Cui, S. Ren, Chem. Mater. 27 (2015) 4677–4681.
[17] T. Chen, W.E. Stutius, IEEE Trans. Magn. 10 (1974) 581–586.
[18] M. Barbic, J. Magn. Magn. Mater. 249 (2002) 357–367.
[19] H. Kronmüller, M. Fähnle, Micromagnetism and the Microstructure of Ferromagnetic Solids, Cambridge University Press, Cambridge, 2003.
[20] H. Kronmüller, in: G.J. Long, F. Grandjean (Eds.), Supermagnets, Hard Magnetic Materials, Kluwer, Dordrecht 1991, p. 461.
[21] H. Kronmüller, J.B. Yang, D. Goll, J. Phys. Condens. Matter 26 (2014) (064210).
[22] C. Curcio, E.S. Olivetti, L. Matino, M. Kupferling, V. Basso, Phys. Procedia 75 (2015) 1230–1237.
[23] S. Kavita, U.M.R. Seelam, D. Prabhu, R. Gopalan, J. Magn. Magn. Mater. 377 (2015) 485–489.
[24] Y.B. Yang, X.G. Chen, S. Guo, A.R. Yan, Q.Z. Huang, M.M. Wu, D.F. Chen, Y.C. Yang, J.B. Yang, J. Magn. Magn. Mater. 330 (2013) 106–110.
[25] V. Ly, X. Wu, L. Smillie, T. Shoji, A. Kato, A. Manabe, K. Suzuki, J. Alloys Compd. 615 (2014) S285–S290.
[26] W. Liu, Y. Liu, R. Skomski, D.J. Sellmyer, in: Y. Liu, D. Sellmyer, D. Shindo (Eds.), Handbook of Advanced Magnetic Materials, Tsinghua University Press-Springer, New York-Beijing 2006, p. 226.
[27] O. Henkel, Phys. Status Solidi 7 (1964) 919.
[28] G. Bertotti, Hysteresis in Magnetism, Academic Press, San Diego, 1998 250.
[29] J. Garcia-Otero, M. Porto, J. Rivas, J. Appl. Phys. 87 (2000) 7376.
[30] J.M.D. Coey, Magnetism and Magnetic Materials, Cambridge University Press, Cambridge, 2010 245.